

Tunable THz surface plasmon polariton based on a topological insulator/layered superconductor hybrid structure

Mingda Li,^{1,*} Zuyang Dai,² Wenping Cui,³ Zhe Wang,¹ Ferhat Katmis,⁴ Jiayue Wang,⁵ Peisi Le,¹ Lijun Wu,⁶ and Yimei Zhu⁶

¹*Department of Nuclear Science and Engineering, Massachusetts Institute of Technology, 77 Massachusetts Avenue, Cambridge, Massachusetts 02139, USA*

²*Department of Physics, Tsinghua University, Beijing 100084, China*

³*Institut für Theoretische Physik, Universität zu Köln, Zùlpicher Straße 77, D-50937 Köln, Germany*

⁴*Department of Physics, Massachusetts Institute of Technology, 77 Massachusetts Avenue, Cambridge, Massachusetts 02139, USA*

⁵*Department of Engineering Physics, Tsinghua University, Beijing 10084, China*

⁶*Department of Condensed Matter Physics, Brookhaven National Lab, Upton, New York 11973, USA*

(Received 6 March 2014; revised manuscript received 5 May 2014; published 25 June 2014)

We theoretically investigate the surface plasmon polariton (SPP) at the interface between a three-dimensional strong topological insulator (TI) and a layered superconductor/magnetic insulator structure, within the random phase approximation. The tunability of the SPP through electronic doping can be enhanced when the magnetic permeability of the layered structure becomes higher. When the interface is gapped by superconductivity or perpendicular magnetism, the SPP dispersion is further distorted, accompanied by a shift of group velocity and penetration depth. Such a shift of the SPP reaches a maximum when the magnitude of the Fermi level approaches the gap value, and may lead to observable effects. The tunable SPP at the interface between layered-superconductor and magnetic materials in proximity to the TI surface may provide new insight in the detection of Majorana fermions.

DOI: [10.1103/PhysRevB.89.235432](https://doi.org/10.1103/PhysRevB.89.235432)

PACS number(s): 73.20.Mf, 73.25.+i

I. INTRODUCTION

Surface plasmon polariton (SPP) is the collective excitation of electrons at the interface between a conductor and dielectrics driven by electromagnetic (EM) waves. [1,2] Despite its wide applications in nanophotonics [3], near-field optics and tip-enhanced Raman spectroscopy [4,5], and biological sensors and antennas [6,7], the SPP in general suffers from problem of huge nonradiative loss due to the strong absorption of the metal [1–4] accompanied by additional radiative loss [8], which limits SPP lifetime and propagation length for further application in integrated devices.

In order to solve the SPP loss problem, low-loss plasmonics based on graphene [9–23] and topological insulators (TIs) [24–31] has attracted much recent attention. In far-infrared and THz range, the major loss mechanism in graphene lies in the scattering between electrons and optical phonons [11]. A number of studies in graphene plasmonics have been conducted utilizing the properties of low loss and tunability. Yan *et al.* [32] have reported enhanced plasmon resonance in a patterned graphene-insulator stack structure when compared with single-layered graphene, while Ju *et al.* [12] demonstrated an enhanced tunability in the THz range in microribbon graphene metamaterials. These efforts target manipulation of photons and miniaturization of optical devices, and could be further integrated and hybridized toward applications in detectors, modulators or other integrated devices.

On the other hand, in a doped three-dimensional (3D) TI, the electron-impurity scattering becomes dominant due to weak electron-phonon coupling [28], with a further reduced

backscattering probability due to topological protected surface states [33–35]. However, unlike the booming studies in graphene plasmonics, plasmon hybrid devices in TIs have been seldom reported, even with comparable performance in the THz range as well as other promising features such as net spin polarization, i.e., “spin plasmon” [24–26,31] and spin-charge separation [30].

Therefore, in this paper, we propose a plasmonic hybrid structure composed of a 3D TI in close contact with a layered superconductor. This structure provides a new platform where SPP waves are supported. The tunability of the SPP propagation can be achieved independently through either gate voltage or external magnetic field. Since the Majorana bound states, which are non-Abelian anyons in superconductors and have great significance in topological quantum computation [34], are predicted to exist at the boundary between a 3D TI and a superconductor, this plasmonic structure may provide a new perspective in search of Majorana bound states.

II. THEORY

A. Dispersion relation of an anisotropic SPP wave

Since the SPP wave is well localized at the interface, while the Dirac electrons only exist on the surface of a TI, we could apply anisotropic dielectric functions to model the dielectric function of a 3D TI in order to capture both the dielectric function of surface 2D chiral Dirac electrons (Fig. 1, x,y plane, $z = 0$) and the bulk dielectric constant (Fig. 1, $z > 0$ region).

In order to describe wave propagation in the layered structure (Fig. 1, $z < 0$ region), we adopt the method proposed by Averkov *et al.* [36] using an anisotropic dielectric function. This is valid when $\lambda_{SP} \gg D$, where λ_{SP} is the SPP wavelength, and D is the spatial periodicity of the layered structure. Since

*Author to whom correspondence should be addressed: mingda@mit.edu

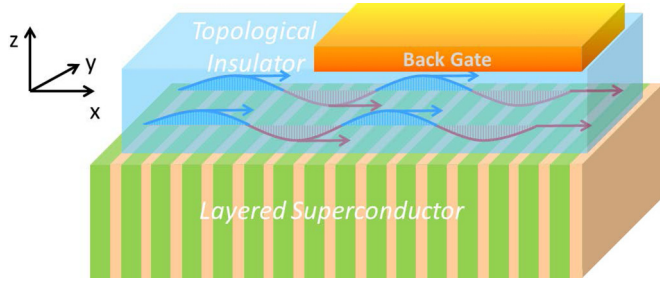


FIG. 1. (Color online) The schematic configuration of a 3D TI/layered superconductor hybrid structure. The $z < 0$ region consists of alternating layers of superconductor and insulator. The SPP wave propagates along the interface. A back gate is present to tune the Fermi level of the interfacial electrons, which leads to a change of dielectric functions and furthermore a change of SPP propagation properties.

we are interested in the long-wavelength THz range, the condition $\lambda_{\text{SP}} \gg D$ is guaranteed to be met. In this approach, the anisotropy leads to the existence of an optical axis where the EM wave suffers no birefringence [37]. Thus the electric field and magnetic field at the interface can be written as a superposition of an ordinary wave and an extraordinary wave:

$$\begin{aligned} \mathbf{E}_j &= (\mathbf{E}_j^o e^{-\kappa_j^o |z|} + \mathbf{E}_j^e e^{-\kappa_j^e |z|}) e^{i(q_x x + q_y y - \omega t)}, \\ \mathbf{H}_j &= (\mathbf{H}_j^o e^{-\kappa_j^o |z|} + \mathbf{H}_j^e e^{-\kappa_j^e |z|}) e^{i(q_x x + q_y y - \omega t)}, \end{aligned} \quad (1)$$

where $j = 1, 2$ denote the TI and layered superconductor sides, respectively. Based on our model, the TI dielectric function is defined as $\varepsilon_1 = (\varepsilon_{2D}(q, \omega), \varepsilon_{2D}(q, \omega), \varepsilon_d)$ with optical axis along the z direction, while the dielectric function of the layered superconductor is defined as $\varepsilon_2 = (\varepsilon_c(\omega), \varepsilon_{ab}(\omega), \varepsilon_{ab}(\omega))$, which is anisotropic along the x direction.

Noticing the different directions of optical axis in the upper TI region and lower superconductor region, then for ordinary wave and extraordinary wave we have $E_{1z}^o = 0$, $E_{2x}^o = 0$ and $H_{1z}^e = 0$, $H_{2x}^e = 0$, respectively. These equalities are valid approximately, since, when the gap is opened, the electromagnetic constitutive relation is modified to incorporate the topological magnetoelectric effect [38],

$$\begin{aligned} \mathbf{D} &= \varepsilon \mathbf{E} - \frac{\varepsilon_0 c \alpha \theta}{\pi} \mathbf{B} \\ \mathbf{H} &= \frac{1}{\mu} \mathbf{B} + \frac{\alpha \theta}{c \mu_0 \pi} \mathbf{E} \end{aligned} \quad (2)$$

However, despite the $O(\alpha)$ correction to the electromagnetic field by this axion constitutive relation, it actually contributes only an order of $O(\alpha^2) \sim 10^{-4}$ correction to the plasmon energy [38]. Moreover, since we are interested in the relative SPP energy shift upon gating or gapping, but not the absolute magnitude of SPP energy, the contribution from the axion term will be canceled out when calculating the energy difference, since the ungated or gapless SPP energy already contains the contribution from the axion term [39]. Thus, compared with the huge energy shift ($\sim 1\%$ originated from gapping or doping) in all following calculations, we could safely neglect the axion term and set $\alpha = 0$. Within this approximation, the components of the EM fields are shown in Appendix A, with

light speed in vacuum $c = 1$ and μ is the magnetic permeability of the layered superconductor material.

Substituting the EM field components back into Eq. (1), we obtain the localization constants, i.e., the inverse of penetration depth away from the interface.

$$\begin{aligned} \kappa_1^o &= \sqrt{q_x^2 + q_y^2 - \varepsilon_{2D}(q, \omega) \omega^2}, \\ \kappa_1^e &= \sqrt{\varepsilon_{2D}(q, \omega) \left(\frac{q_x^2 + q_y^2}{\varepsilon_d} - \omega^2 \right)}, \\ \kappa_2^o &= \sqrt{q_x^2 + q_y^2 - \mu \varepsilon_{ab}(q, \omega) \omega^2}, \\ \kappa_2^e &= \sqrt{\frac{\varepsilon_c(q, \omega)}{\varepsilon_{ab}(q, \omega)} q_x^2 + q_y^2 - \mu \varepsilon_c(q, \omega) \omega^2}. \end{aligned} \quad (3)$$

The dispersion relation of the resulting surface wave can be written in a determinant form:

$$\begin{vmatrix} -i\kappa_1^o & \frac{i\omega^2 \varepsilon_1}{\kappa_1^e} & -\frac{q_y^2 - (\kappa_2^o)^2}{i\mu \kappa_2^e} & 0 \\ -q_y^2 & q_x^2 & 0 & -q_x^2 + \mu \omega^2 \varepsilon_{ab} \\ \kappa_1^o q_y^2 & \frac{\omega^2 q_x^2 \varepsilon_1}{\kappa_1^e} & \frac{q_x^2 q_y^2}{\mu \kappa_2^e} & \omega^2 \varepsilon_{ab} \kappa_2^e \\ 1 & 1 & -1 & -1 \end{vmatrix} = 0 \quad (4)$$

In this paper, we only consider the wave propagating along the x direction, neglecting the oblique excitation. The dispersion relation can finally be simplified as

$$q = \omega \sqrt{\frac{\varepsilon_d \varepsilon_{ab}(\omega) [\varepsilon_c(\omega) - \mu \varepsilon_{2D}(q, \omega)]}{\varepsilon_c(\omega) \varepsilon_{ab}(\omega) - \varepsilon_{2D}(q, \omega) \varepsilon_d}} \quad (5)$$

which is the main analytical result. In this expression, μ is the effective permeability of the layered superconductor structure and q is the wave number along the x direction, and can be a complex number. When both the upper and lower materials are isotropic, i.e., $\varepsilon_{2D} = \varepsilon_d = \varepsilon_1$ and $\varepsilon_{ab} = \varepsilon_c = \varepsilon_2$, it is further reduced to the well known result $q = \omega \sqrt{\frac{\varepsilon_1 \varepsilon_2}{\varepsilon_1 + \varepsilon_2}}$.

B. Dielectric function of the layered superconductor

Defining dimensionless frequency $\Omega = \omega/\omega_J$, with ω_J the Josephson plasmon frequency of the layered superconductor, the dielectric function of the layered superconductor can be written as [36]

$$\varepsilon_c(\Omega) = \varepsilon_s \left(1 - \frac{1}{\Omega^2} \right), \quad \varepsilon_{ab}(\Omega) = \varepsilon_s \left(1 - \frac{\gamma^2}{\Omega^2} \right), \quad (6)$$

where the imaginary parts are neglected. Throughout this article, we take the value reported in [36] and set the interlayer dielectric constant $\varepsilon_s = 16$, current-anisotropy parameter $\gamma = 200$, and $\omega_J = 4$ meV.

C. Dielectric function of the gapless topological insulator

The dielectric function of the chiral gapless topological insulator surface has been reported in [24, 25, 27], where, for the Hamiltonian for a 2D helical Dirac electron gas \mathcal{H}_0 ,

$$\mathcal{H}_0 = \hbar v_F \sum_k \Psi_k^\dagger (\hat{z} \times \vec{k}) \cdot \vec{\sigma} \Psi_k, \quad (7)$$

the Lindhard Dielectric function $\varepsilon_{2D}(q, \omega)$ can be written as

$$\varepsilon_{2D}(q, \omega) = 1 - V_{2D}(q)\Pi(q, \omega) = 1 - \frac{e^2}{2\varepsilon_0 q} \Pi(q, \omega) \quad (8)$$

with the polarization operator

$$\begin{aligned} \Pi(q, \omega) &= \frac{g}{4\pi^2} \sum_{\gamma, \gamma'} \int d\mathbf{k} \frac{n_{\mathbf{k}, \gamma} - n_{\mathbf{k}+\mathbf{q}, \gamma'}}{\hbar\omega + E_{\mathbf{k}, \gamma} - E_{\mathbf{k}+\mathbf{q}, \gamma'} + i\delta} \\ &\times |(f_{\mathbf{k}, \gamma} | f_{\mathbf{k}+\mathbf{q}, \gamma'})|^2. \end{aligned} \quad (9)$$

In this expression, g is the spin/valley degeneracy, for the chiral states we have $g = 1$ due to spin-momentum locking, $n_{\mathbf{k}, \gamma}$ is the Fermi occupation value at the energy eigenvalue, and $E_{\mathbf{k}, \gamma} = \gamma \hbar v_F k$, with $\gamma = 1$ for conduction band and $\gamma = -1$ for valence band, respectively. The spinor eigenstates $|f_{\mathbf{k}, \gamma}\rangle = (e^{-i\theta_{\mathbf{k}}/2}, i\gamma e^{i\theta_{\mathbf{k}}/2})/\sqrt{2}$, with $\theta_{\mathbf{k}}$ defined as $\tan \theta_{\mathbf{k}} = k_y/k_x$. We take the value of Fermi velocity $v_F = 6.2 \times 10^5$ m/s [40] in all calculations.

The random-phase approximation (RPA) relaxation time (RT) approximation [41] can be applied to describe the SPP damping along the propagation direction, which leads to a finite propagation length. Defining polarizability $\chi(q, \omega) \equiv \frac{e^2}{q^2} \Pi(q, \omega)$, the renormalized polarizability, taking the conservation of electron number into account, can then be written as

$$\chi_\tau(q, \omega) = \frac{(1 + i/\omega\tau)\chi(q, \omega + i/\tau)}{1 + (i/\omega\tau)\chi(q, \omega + i/\tau)\chi(q, 0)}, \quad (10)$$

where τ is the relaxation time, which is in general frequency dependent, and mainly originates from the electron-phonon coupling, scattering by superconductor quasiparticles, as well as impurities scattering. In this situation, τ can be calculated using electron self-energy [11]:

$$\Sigma(E) = \Sigma_{e-ph}(E) + \Sigma_{sc}(E) + \Sigma_{imp}(E) \quad (11)$$

When the SPP frequency is higher than the gap of the superconductor or above the optical frequency of the topological insulator, the self-energy in Eq. (11) contains a prominent imaginary part, which leads to a drastic reduction of propagation length. However, since we are interested in low-frequency SPPs ($\omega < \omega_J = 4$ meV, shown in Fig. 2), where only impurity scattering dominates, the relaxation time can be directly written as $\tau = \mu \hbar \sqrt{n\pi} / e v_F$, without the need of implementing Eq. (11). Since $\tau \sim 10^{-12}$ s is a very large

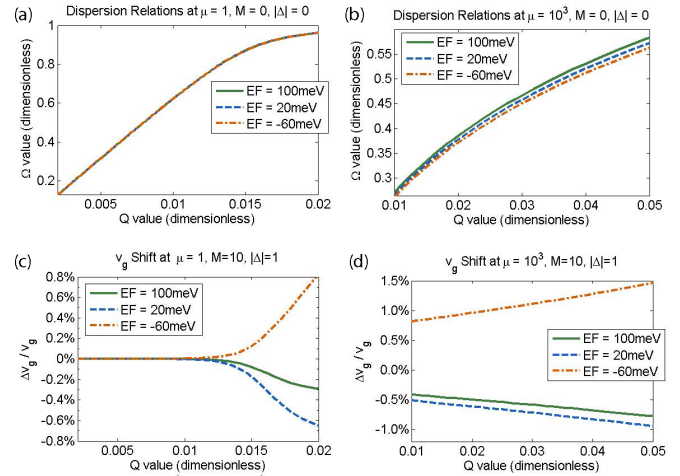


FIG. 2. (Color online) The dispersion relations (a),(b) and gap-induced group velocity changes (c),(d) of the SPP at various Fermi levels with respect to gap opening. The Fermi levels are taken at three different values with 80 meV intervals. In (c), at $\mu = 1$, even if the tuning of the Fermi level does not change much relative to the dispersion relation shown in (a), it still shows a shift to the SPP group velocity in the high- Q range.

quantity, and moreover we are interested in the frequency and the tunability of the SPP but not the exact propagation length, for simplicity we take $\tau = \infty$ in all following calculations, using Eq. (9) instead of Eq. (10).

Equation (9) can be calculated either analytically [10,27] or numerically, thanks to the identical expression of the polarization operator within the RPA for a simple Dirac gas and a helical Dirac gas. In our approach, we choose $T = 10$ K for numerical integration to avoid discontinuity, and compare with analytical result with at least six-digit agreement. Then the numerical result for the gapless TI is applied to solve for the dielectric function of the TI when the surface state is gapped.

D. Dielectric function of the gapped topological insulator

Either the magnetic field perpendicular to the interface (z direction in Fig. 1) or the superconductivity would open up a gap to the gapless Dirac cone, and lift out the degeneracy at $k = 0$, and further alter the dielectric function as well as SPP dispersions. In order to take into account the effect of gaps, we adopt the Bogoliubov–de Gennes Hamiltonian [33,42], which can be regarded as a generalization of Eq. (7):

$$\mathcal{H}_{BdG} = \frac{1}{2} \sum_{\mathbf{k}} \Psi_{\mathbf{k}}^{\dagger} \begin{pmatrix} k_x \sigma_y - k_y \sigma_x + M \sigma_z - E_F & i|\Delta| \sigma_y \\ -i|\Delta| \sigma_y & -k_x \sigma_y - k_y \sigma_x - M \sigma_z - E_F \end{pmatrix} \Psi_{\mathbf{k}}, \quad (12)$$

where spinor $\Psi_{\mathbf{k}} = (c_{\mathbf{k}\uparrow}, c_{\mathbf{k}\downarrow}, c_{-\mathbf{k}\uparrow}^{\dagger}, c_{-\mathbf{k}\downarrow}^{\dagger})$, M and $|\Delta|$ denote the magnetic gap and superconductivity gap, respectively, and E_F is the chemical potential. Both Eqs. (8) and (9) still hold, but the eigenvalues and eigenvectors are changed. The eigenvalues can now be written as

$$\begin{aligned} E_1 &= \sqrt{|\Delta|^2 + 2(|\Delta|^2 M^2 + E_F^2 M^2 + E_F^2 k^2)^{1/2} + M^2 + k^2 + E_F^2}, \\ E_2 &= \sqrt{|\Delta|^2 - 2(|\Delta|^2 M^2 + E_F^2 M^2 + E_F^2 k^2)^{1/2} + M^2 + k^2 + E_F^2}, \end{aligned}$$

$$E_3 = -\sqrt{|\Delta|^2 - 2(|\Delta|^2 M^2 + E_F^2 M^2 + E_F^2 k^2)^{1/2} + M^2 + k^2 + E_F^2},$$

$$E_4 = -\sqrt{|\Delta|^2 + 2(|\Delta|^2 M^2 + E_F^2 M^2 + E_F^2 k^2)^{1/2} + M^2 + k^2 + E_F^2}.$$

The corresponding unnormalized eigenvectors are shown in Appendix B.

III. RESULTS AND DISCUSSIONS

In order to conveniently express the dielectric functions for both the TI and layered superconductor, we define dimensionless wave number $Q = v_F q_x / (c\omega_J)$, and all energies are dimensionless and expressed in units of ω_J .

The SPP dispersion relations are obtained by solving Eq. (5). The typical dispersion relations at various gate voltages, i.e., Fermi levels E_F , are shown in Figs. 2(a) and 2(b). We see an enhanced tunability, i.e., a shift of dispersion relation when E_F varies, when the lower layer has increased effective magnetic permeability μ . By defining the SPP group velocity $v_g = d\Omega/dQ$, we see an additional change of propagation properties induced by either M or $|\Delta|$ [Figs. 2(c) and 2(d)] by plotting the percentage SPP group velocity shift,

$$\frac{\Delta v_g}{v_g} = \frac{v_g(\text{gapped}) - v_g(\text{gapless})}{v_g(\text{gapless})}.$$

Here both the magnetic gap M and superconductivity gap $|\Delta|$ are dimensionless in units of the Josephson plasmon frequency ω_J .

In order to further investigate the effect of the gap on the SPP propagation, the relative shift of group velocity $\Delta v_g/v_g$ as a function of dimensionless wave number Q and Fermi

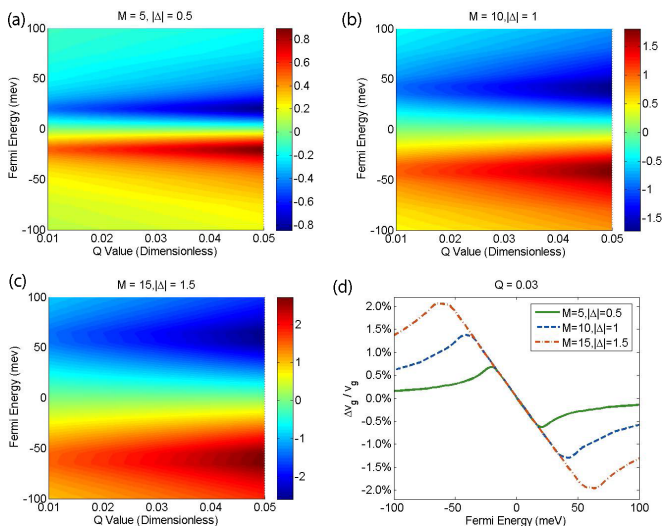


FIG. 3. (Color online) The percentage shift of SPP group velocity as a function of Q and E_F , at three different gap values $M = 5$, $|\Delta| = 0.5$ (a); $M = 10$, $|\Delta| = 1.0$ (b); and $M = 15$, $|\Delta| = 1.5$ (c). The change is negative for $E_F > 0$ and positive for $E_F < 0$, and reaches a maximum when the Fermi level is close to the gap values (d). Notice all gap values are expressed in units of ω_J ($\omega_J = 4$ meV throughout the calculation); for instance the green solid line $M = 5$, $|\Delta| = 0.5$ corresponds to $M = 20$ meV, $|\Delta| = 2$ meV.

level E_F is shown in Fig. 3, at different values of gap. It can be seen directly that the shift is increased at larger gap value, and it increases as a function of Q . Most importantly, the shift reaches a peak value when the Fermi level approaches the gap value. This feature can be seen more clearly in a line plot with fixed Q value [Fig. 3(d)]. We also see that SPP group velocity v_g does not shift when Fermi level $E_F = 0$. In contrast to the Q and E_F dependent shift of group velocity caused by the energy gap, the localization constants show a qualitatively different behavior. The localization constant in the TI side κ_1^o is sensitive neither to E_F nor to Q [Figs. 4(a), 4(c), and 4(e)], while in the layered superconductor side κ_2^o is tunable by E_F but still Q independent. The importance of the localization constant shift with Q can hardly be overestimated, in that it indicates that the different propagation properties of the SPP are almost fully coming from the group velocity, other than the difference in SPP wavelength. Fewer controllable variables would definitely make the experimental results easier to explain.

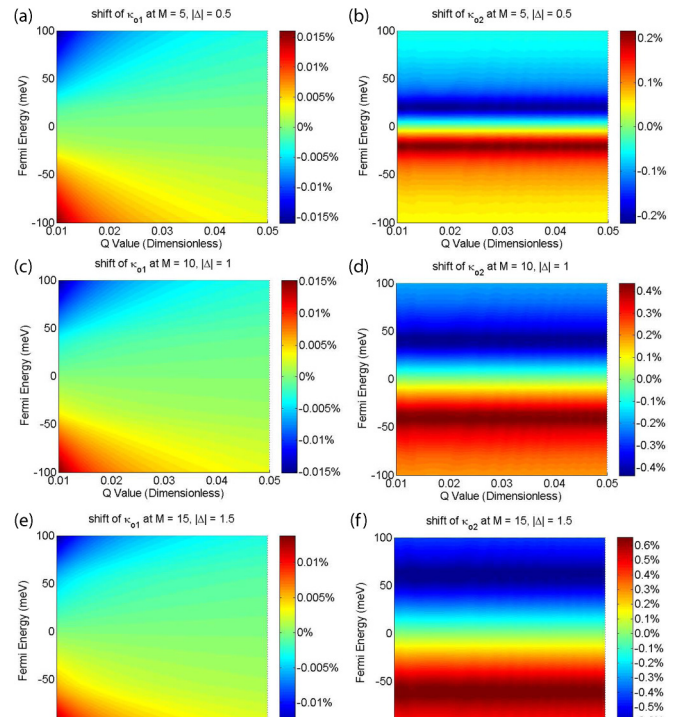


FIG. 4. (Color online) Relative shift of the o -light component of localization constants for TI κ_1^o [panels (a), (c), (e)], and layered superconductor κ_2^o [panels (b), (d), (f)]. The localization constants for e -light κ_1^e and κ_2^e have different magnitudes but features similar to κ_1^o and κ_2^o , respectively. We see that the shift is not sensitive to the Fermi level E_F of topological insulators, but always reaches peak values when E_F is near the value of the gap. Unlike the shift of group velocity, which is Q dependent, the localization constants are almost independent of Q value.

The reason that the maximum v_g shift occurs when the gap matches the Fermi level can be understood in the light of electronic transition and available electron density for plasmonic oscillation. Electrons in the conduction band are mostly extended and dominate the surface plasmon excitation. When the Fermi level is lower than the energy gap, charge carriers need additional energy to fulfill the transition to the conduction band in order to contribute to the collective excitation. On the other hand, since the SPP is excited by EM waves, when the Fermi level is higher than the energy gap, the electronic transition by optical excitation is limited by occupied electrons. The increasing forbidden transition leads to a reduced shift of dielectric function, and moreover the v_g shift is reduced accordingly. Thus, only when the Fermi level reaches the value of energy gap is the number of available electrons participating in the electronic transition and collective excitation maximized, and leads to a shift of SPP frequency and group velocity.

IV. CONCLUSIONS

We provide a generic theoretical framework to study the surface plasmon polariton (SPP) at the interface between a topological insulator (TI) and layered superconductors. The SPP in this hybrid structure may be widely applied to study novel optical and transport phenomena at the interface, through the tunability of SPP propagation by gating or gapping the surface states of the TI. It can also be generalized to a larger category of materials in proximity to a TI surface. For instance, Wei *et al.* [43,44] have shown that when the ferromagnetic insulator EuS is on the top of topological insulator Bi₂Se₃, it induces significant magnetic moment in Bi₂Se₃ thin films and induces breaking of T -reversal symmetry. The SPP in such a ferromagnetic/TI hybrid structure can also be studied within this approach.

Furthermore, the Majorana zero mode is predicted to exist [35,42,45] as a domain wall state at the interface between TI and ferromagnetic-superconductor boundaries. Therefore, at the TI/layered superconductor interface, propagating SPPs may interact with the Majorana domain wall state, and lead to the shift of the SPP propagation properties, including group velocity, reflectivity and transmissivity, etc. In this regard, the change of optical properties of the SPP can be considered a semiclassical manifestation of the existence of Majorana fermions, which is a pure quantum phenomenon with non-Abelian statistics. The existence of the zero-mode level may contribute to electronic transition, and leads to a further change of dielectric functions. Unlike transport measurements, which involve only a single Majorana fermion domain wall state, this hybrid structure can be regarded as the interaction between the SPP and a series of domain wall states, coming from each domain wall state along the interface. In a nutshell, the SPP on the TI surface may provide insights to the detection of Majorana Fermions as a conceptually novel platform.

ACKNOWLEDGMENTS

Author Mingda Li would thank Prof. Ju Li for his generous support and helpful discussions.

APPENDIX A: COMPONENTS OF EM FIELDS

$$\begin{aligned}
 H_{1x}^o &= \frac{\kappa_1^o}{i\omega} E_{1y}^o, & E_{1x}^o &= -\frac{q_y}{q_x} E_{1y}^o, & H_{1y}^o &= -\frac{i\kappa_1^o q_y}{\omega q_x} E_{1y}^o, \\
 H_{1z}^o &= \frac{q_x^2 + q_y^2}{\omega q_x} E_{1y}^o, & H_{1x}^e &= \frac{i\omega \varepsilon_{2D}(q, \omega)}{\kappa_1^e} E_{1y}^e, \\
 E_{1x}^e &= \frac{q_x}{q_y} E_{1y}^e, \\
 H_{1y}^e &= -\frac{i\omega q_x \varepsilon_{2D}(q, \omega)}{q_y \kappa_1^e} E_{1y}^e, \\
 E_{1z}^e &= \left(\frac{i\kappa_1^e}{q_y} + \frac{i\omega^2 \varepsilon_{2D}(q, \omega)}{q_y \kappa_1^e} \right) E_{1y}^e, \\
 H_{2z}^o &= \frac{q_x}{\omega \mu} E_{2y}^o, & H_{2y}^o &= \frac{i q_x q_y}{\omega \mu \kappa_2^o} E_{2y}^o, & E_{2z}^o &= -\frac{i q_y}{\kappa_2^o} E_{2y}^o, \\
 H_{2x}^o &= \frac{q_y^2 - (\kappa_2^o)^2}{i\omega \mu \kappa_2^o} E_{2y}^o, & E_{2z}^e &= \frac{\kappa_2^e}{i q_y} E_{2y}^e, \\
 H_{2z}^e &= \frac{\omega \varepsilon_{ab}(q, \omega)}{q_x} E_{2y}^e, \\
 H_{2y}^e &= -\frac{\omega \varepsilon_{ab}(q, \omega) \kappa_2^e}{i q_x q_y} E_{2y}^e, & E_{2x}^e &= \frac{q_x^2 - \mu \omega^2 \varepsilon_{ab}(q, \omega)}{q_x q_y} E_{2y}^e,
 \end{aligned}$$

APPENDIX B: (UNNORMALIZED) EIGENVECTORS OF THE BdG HAMILTONIAN

Defining $k^2 = k_x^2 + k_y^2$, $\delta^- = |\Delta| - M$, and $\delta^+ = |\Delta| + M$, the four eigenvectors can be written as

$$\begin{aligned}
 |f_{\mathbf{k},1}\rangle &= \left(-1, \frac{\delta^- + \sqrt{(\delta^-)^2 + k^2}}{i k_x + k_y}, -\frac{\delta^- + \sqrt{(\delta^-)^2 + k^2}}{i k_x + k_y}, 1 \right)^T, \\
 |f_{\mathbf{k},2}\rangle &= \left(1, \frac{\delta^+ - \sqrt{(\delta^+)^2 + k^2}}{i k_x + k_y}, \frac{\delta^+ - \sqrt{(\delta^+)^2 + k^2}}{i k_x + k_y}, 1 \right)^T, \\
 |f_{\mathbf{k},3}\rangle &= \left(-1, \frac{\delta^- - \sqrt{(\delta^-)^2 + k^2}}{i k_x + k_y}, \frac{-\delta^- + \sqrt{(\delta^-)^2 + k^2}}{i k_x + k_y}, 1 \right)^T, \\
 |f_{\mathbf{k},4}\rangle &= \left(1, \frac{\delta^+ + \sqrt{(\delta^+)^2 + k^2}}{i k_x + k_y}, \frac{\delta^+ + \sqrt{(\delta^+)^2 + k^2}}{i k_x + k_y}, 1 \right)^T.
 \end{aligned}$$

- [1] J. Pitarke, V. Silkin, E. Chulkov, and P. Echenique, *Rep. Prog. Phys.* **70**, 1 (2007).
 [2] S. A. Maier, *Plasmonics: Fundamentals and Applications: Fundamentals and Applications* (Springer, Berlin, 2007).

- [3] *Surface Plasmon Nanophotonics*, edited by P. G. Kik and M. L. Brongersma, Springer Series in Optical Sciences Vol. 131 (Springer, Dordrecht, 2007).

- [4] *Near-Field Optics and Surface Plasmon Polaritons*, edited by S. Kawata, M. Ohtsu, and M. Irie, Topics in Applied Physics Vol. 81 (Springer, Berlin, 2001).
- [5] W. Cui, M. Li, Z. Dai, Q. Meng, and Y. Zhu, *J. Chem. Phys.* **140**, 044109 (2014).
- [6] *Surface Plasmon Resonance Based Sensors*, edited by J. Homola, Springer Series on Chemical Sensors and Bio Sensors Vol. 4 (Springer, Berlin, 2006).
- [7] J. Becker, *Plasmons as Sensors* (Springer, Berlin, 2012).
- [8] T. Vary and P. Markos, *Opto-Electronics Rev.* **18**, 400 (2010).
- [9] B. Wunsch, T. Stauber, F. Sols, and F. Guinea, *New J. Phys.* **8**, 318 (2006).
- [10] E. H. Hwang and S. Das Sarma, *Phys. Rev. B* **75**, 205418 (2007).
- [11] M. Jablan, H. Buljan, and M. Soljacic, *Phys. Rev. B* **80**, 245435 (2009).
- [12] L. Ju, B. Geng, J. Horng, C. Girit, M. Martin, Z. Hao, H. A. Bechtel, X. Liang, A. Zettl, Y. R. Shen *et al.*, *Nat. Nanotechnol.* **6**, 630 (2011).
- [13] F. H. Koppens, D. E. Chang, and F. J. Garcia de Abajo, *Nano Lett.* **11**, 3370 (2011).
- [14] H. Yan, F. Xia, Z. Li, and P. Avouris, *New J. Phys.* **14**, 125001 (2012).
- [15] A. Grigorenko, M. Polini, and K. Novoselov, *Nat. Photonics* **6**, 749 (2012).
- [16] S. A. Maier, *Nat. Phys.* **8**, 581 (2012).
- [17] Q. Bao and K. P. Loh, *ACS Nano* **6**, 3677 (2012).
- [18] P. Tassin, T. Koschny, M. Kafesaki, and C. M. Soukoulis, *Nat. Photonics* **6**, 259 (2012).
- [19] V. W. Brar, M. S. Jang, M. Sherrott, J. J. Lopez, and H. A. Atwater, *Nano Lett.* **13**, 2541 (2013).
- [20] D. Jin, A. Kumar, K. H. Fung, J. Xu, and N. X. Fang, *Appl. Phys. Lett.* **102**, 201118 (2013).
- [21] W. B. Lu, W. Zhu, H. J. Xu, Z. H. Ni, Z. G. Dong, and T. J. Cui, *Opt. Express* **21**, 10475 (2013).
- [22] H. Buljan, M. Jablan, and M. Soljacic, *Nat. Photonics* **7**, 346 (2013).
- [23] P. Avouris and M. Freitag, *IEEE Journal of Selected Topics in Quantum Electronics* **20**, 72 (2014).
- [24] D. K. Efimkin, Y. E. Lozovik, and A. A. Sokolik, *Nanoscale Res. Lett.* **7**, 1 (2012).
- [25] D. Efimkin, Y. E. Lozovik, and A. Sokolik, *J. Magn. Magn. Mater.* **324**, 3610 (2012).
- [26] O. Roslyak, G. Gumbs, and D. Huang, *Phys. Rev. B* **87**, 045121 (2013).
- [27] R. Schutky, C. Ertler, A. Trugler, and U. Hohenester, *Phys. Rev. B* **88**, 195311 (2013).
- [28] P. Di Pietro, M. Ortolani, O. Limaj, A. Di Gaspare, V. Giliberti, F. Giorgianni, M. Brahlek, N. Bansal, N. Koirala, S. Oh *et al.*, *Nat. Nanotechnol.* **8**, 556 (2013).
- [29] Y. Okada and V. Madhavan, *Nat. Nanotechnol.* **8**, 541 (2013).
- [30] T. Stauber, G. Gomez-Santos, and L. Brey, *Phys. Rev. B* **88**, 205427 (2013).
- [31] C. Chen, Z. Xie, Y. Feng, H. Yi, A. Liang, S. He, D. Mou, J. He, Y. Peng, X. Liu *et al.*, *Sci. Rep.* **3**, 2411 (2013).
- [32] H. Yan, X. Li, B. Chandra, G. Tulevski, Y. Wu, M. Freitag, W. Zhu, P. Avouris, and F. Xia, *Nat. Nanotechnol.* **7**, 330 (2012).
- [33] B. A. Bernevig, *Topological Insulators and Topological Superconductors* (Princeton University Press, Princeton, 2013).
- [34] M. Z. Hasan and C. L. Kane, *Rev. Mod. Phys.* **82**, 3045 (2010).
- [35] X.-L. Qi and S.-C. Zhang, *Rev. Mod. Phys.* **83**, 1057 (2011).
- [36] Y. O. Averkov, V. M. Yakovenko, V. A. Yampol'skii, and F. Nori, *Phys. Rev. B* **87**, 054505 (2013).
- [37] E. Hecht, *Optics*, 4th ed. (Addison Wesley Longman Inc., San Francisco, 1998), Vol. 1.
- [38] A. Karch, *Phys. Rev. B* **83**, 245432 (2011).
- [39] M. Li, W. Cui, L. Wu, Q. Meng, Y. Zhu, Y. Zhang, W. Liu, and Z. Ren, *arXiv:1309.6198*.
- [40] H. Zhang, C.-X. Liu, X.-L. Qi, X. Dai, Z. Fang, and S.-C. Zhang, *Nat. Phys.* **5**, 438 (2009).
- [41] N. D. Mermin, *Phys. Rev. B* **1**, 2362 (1970).
- [42] L. Fu and C. L. Kane, *Phys. Rev. Lett.* **100**, 096407 (2008).
- [43] P. Wei, F. Katmis, B. A. Assaf, H. Steinberg, P. Jarillo-Herrero, D. Heiman, and J. S. Moodera, *Phys. Rev. Lett.* **110**, 186807 (2013).
- [44] P. Wei, F. Katmis, B. Assaf, D. Heiman, and J. S. Moodera, in *APS Meeting Abstracts*, Vol. 58(1) (2013), p. 13007.
- [45] L. Fu and C. L. Kane, *Phys. Rev. Lett.* **102**, 216403 (2009).